Colloid Polym Sci (2002) 280:446–453
DOI 10.1007/s00396-001-0631-6

ORIGINAL CONTRIBUTION

**Tsuneo Okubo**
**Hisanori Ishiki**
**Hiroshi Kimura**
**Megumi Chiyoda**
**Kohji Yoshinaga**

# Rigidity of colloidal crystals of silica spheres modified with polymers on their surfaces in organic solvents

Received: 10 April 2001
Accepted: 7 November 2001
Published online: 28 March 2002


T. Okubo (✉) · H. Ishiki · H. Kimura
Department of Applied Chemistry and Graduate School of Materials Science
Gifu University, Gifu 501–1193, Japan
E-mail: okubotsu@apchem.gifu-u.ac.jp

M. Chiyoda · K. Yoshinaga
Department of Material Science
Kyusyu Institute of Technology
Kitakyusyu 804-0015, Japan

**Abstract** Rigidity ($G$) of colloidal crystals in organic solvents of acetonitrile and nitrobenzene has been measured by reflection spectroscopy in sedimentation equilibrium. The colloidal spheres used are the silica spheres (136 nm in diameter) modified on their surfaces with polymers, poly(maleic anhydride-*co*-styrene) [P(MA-ST)], poly(methyl methacrylate) (PMMA), or polystyrene (PST). Log $G$ increases linearly with the slope of unity as log $N$ (number density of colloidal spheres) increases. The mean values of the $b$-factor, which is the fluctuation parameter in crystal lattices and should be smaller than 0.1 according to the Lindeman's rule, are $0.045 \pm 0.003$, $0.039 \pm 0.007$, and $0.038 \pm 0.003$ for P(MA-ST)/$SiO_2$, PMMA/$SiO_2$, and PST/$SiO_2$, respectively. These values are larger than that of colloidal crystals of mother silica spheres in the deionized aqueous suspension, 0.028. These results support the important role of the *excluded volume effects from the polymer layers* formed around the silica surfaces. However, contribution of the *excluded volume effects from the electrical double layers* formed around the spheres in the organic solvents is also effective in the colloidal crystallization.

**Keywords** Colloidal crystal · Silica spheres modified with polymers · Rigidity · Excluded volume effect · Reflection spectroscopy · Organic solvent

## Introduction

Recently, keen attention has been paid to colloidal crystals, i.e., crystal-like distribution of colloidal particles in suspensions of aqueous and organic solvents [1, 2, 3, 4, 5, 6, 7, 8, 9, 10, 11, 12, 13]. Many researchers have studied inter-particle interaction, lattice structure, morphology of single crystals, phase transition, crystallization kinetics of nucleation and crystal growth, physico-chemical properties (rigidity, viscosity, etc.), structural changes induced by the external fields such as gravity, centrifugal and electric fields, shearing forces, for example.

Colloidal crystallization takes place with monodispersed colloidal particles in suspension. Many researchers have clarified that the colloidal crystals are formed mainly by Brownian movement of colloidal sized particles resulting in inter-particle *repulsion* by the principle of *minimizing dead space* which is not occupied by the particles [11, 14, 15, 16, 17]. In other words, all the particles assume crystal-like distribution automatically with the help of Brownian movement of the particles in order to *maximize packing density*.

When the extra repulsive interactions like *excluded volume effects* from (a) the *electrical double layers* accompanied with the inter-particle electrostatic repulsion and/or from (b) the *layers absorbed physically or attached chemically* around spheres exist among the colloidal particles, colloidal crystallization takes place easily even at very low particle concentrations. In our

previous papers the rigidities of colloidal crystals have been studied in aqueous suspensions [18, 19, 20, 21, 22, 23, 24, 25, 26, 27, 28, 29, 30, 31, 32, 33] and also in organic or aqueous organic solvents [34, 35]. However, most of the reports have discussed the excluded volume effects from the electrical double layers only, and those from the extra polymer layers have not been studied so often [36, 37].

In this work, rigidities of the colloidal crystals of silica spheres coated with the layers of polymers bound chemically on their surfaces are studied in the organic solvents of acetonitrile or nitrobenzene in order to clarify the contribution of the *excluded volume effects* separately as possible in colloidal crystallization.

## Materials and method

*Materials*. Monodispersed colloidal silica spheres in ethanol suspension, 23 wt% $SiO_2$ and 136 nm in diameter, were kindly donated by Catalysts & Chemicals Ind. Co., Japan. The method of preparation of trimethoxysilylated poly(maleic anhydride-*co*-styrene), P(MA-ST)-Si(OMe)$_3$, trimethoxysilylated poly(methyl methacrylate), PMMA-Si(OMe)$_3$, and trimethoxysilylated polystyrene, PST-Si(OMe)$_3$ have been reported previously [38]. To prepare the P(MA-ST)-modified silica spheres, colloidal silica suspension (20 $cm^3$) was added to a mixture of 3.5 g P(MA-ST)-Si(OMe)$_3$ in 300 $cm^3$ 1,2-dimethoxyethane and 20 $cm^3$ tetrahydrofuran. The suspension was stirred at 90 °C, and then 300 $cm^3$ solvent was removed by azeotropic distillation. Centrifugal separation from the suspension and drying under reduced pressure gave the composite P(MA-ST)/$SiO_2$. IR (KBr): 2950 ($\nu_{C\text{-}H}$), 1857 and 1789 ($\nu_{C=O}$), 1602 ($\nu_{C=C}$), and 1130 ($\nu_{Si\text{-}O}$) $cm^{-1}$. PMMA/$SiO_2$ and PST/$SiO_2$ spheres were prepared by the reaction of PMMA-Si(OMe)$_3$ or PST-Si(OMe)$_3$ with the colloidal silica spheres in the same manner in a previous paper [38]. IR (KBr) for PST/$SiO_2$: 3025 ($\nu_{C\text{-}H}$, phenyl), 2921 ($\nu_{C\text{-}H}$), 1601 and 1581 ($\nu_{C=C}$), 1130 ($\nu_{Si\text{-}O}$) $cm^{-1}$. IR (KBr) for PMMA/$SiO_2$: 2923 ($\nu_{C\text{-}H}$), 1753 ($\nu_{C=O}$), and 1456 ($\delta_{C\text{-}H}$) $cm^{-1}$. Infrared spectra were recorded by a diffuse reflection method on JEOL IR-5500. Number-average molecular weight of polymer ($M_n$) was determined by gel permeation chromatography, calibrated by the polystyrene standard, using tetrahydrofuran as an eluent. Amount of the polymer on the surfaces of the mother silica spheres, PA was determined by the weight decrease during temperature elevation from 100 °C to 800 °C on the thermal analysis.

Acetonitrile and nitrobenzene are the purest grade reagents available commercially and used without further purification and deionization.

*Reflection spectroscopy*. Pyrex vials (2-ml, 9 mm in outside diameter, 35 mm high) with screw caps were used as the cells of the reflection spectrum measurements. The cells were left to stand for one to two months after inverted mixing. The reflection spectra taken through the cell wall at various heights at an incident angle of 90° were recorded on a multichannel photo-detector (MCPD-110B, Otsuka Electronics, Hirakata, Osaka-pref.) connected to a Y-type optical-fiber cable. The instrument was operated by a microcomputer (MC800, Otsuka Electronics).

## Results and discussion

### Reflection spectroscopy in sedimentation equilibrium

Figures 1, 2, and 3 show the typical examples of the height dependences of the reflection spectra in sedimentation equilibrium for P(MA-ST)/$SiO_2$ in acetonitrile, PMMA/$SiO_2$ in acetonitrile, and PST/$SiO_2$ in nitrobenzene, respectively. All the suspensions displayed brilliant iridescent colors and the crystallites began to flicker within several minutes after the suspensions were prepared in the observation cells. The state of the sedimentation equilibrium achieved 21 days after the suspensions were set in the observation cells. Clearly, the reflection peak wavelengths increased as the height increased and all the colloidal crystals were compressed under the gravitational field.

Generally speaking, the shape of a reflection spectrum profile of colloidal crystals is a single peak, a

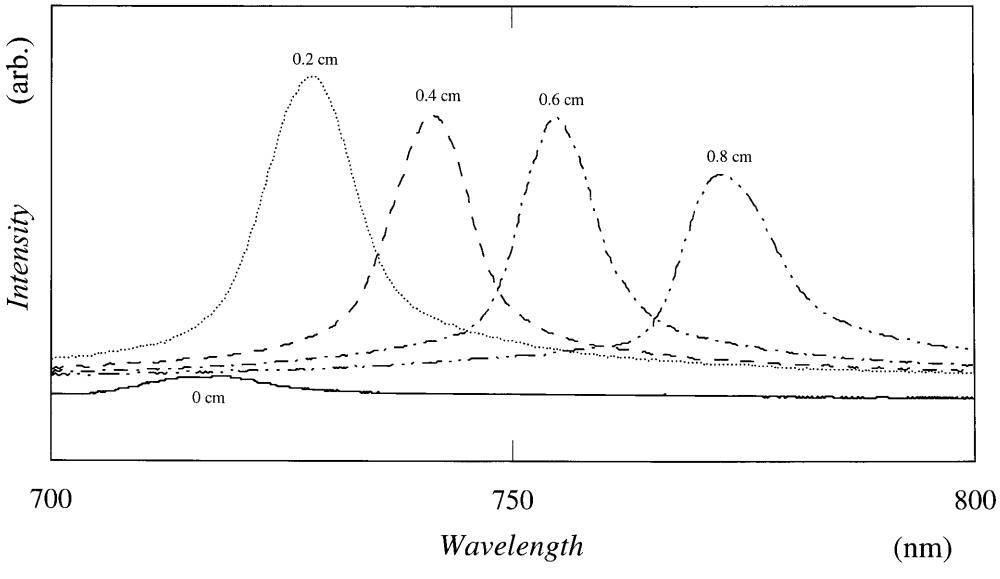


**Fig. 1** Height dependence in the reflection spectra of colloidal crystals of P(MA-ST)/$SiO_2$ spheres in acetonitrile and in a sedimentation equilibrium at 25 °C. 21 days after setting the suspension, $\phi = 0.0408$, $M_n = 6700$. Amount of the polymer attached $(PA) = 80$ mg/g$SiO_2$

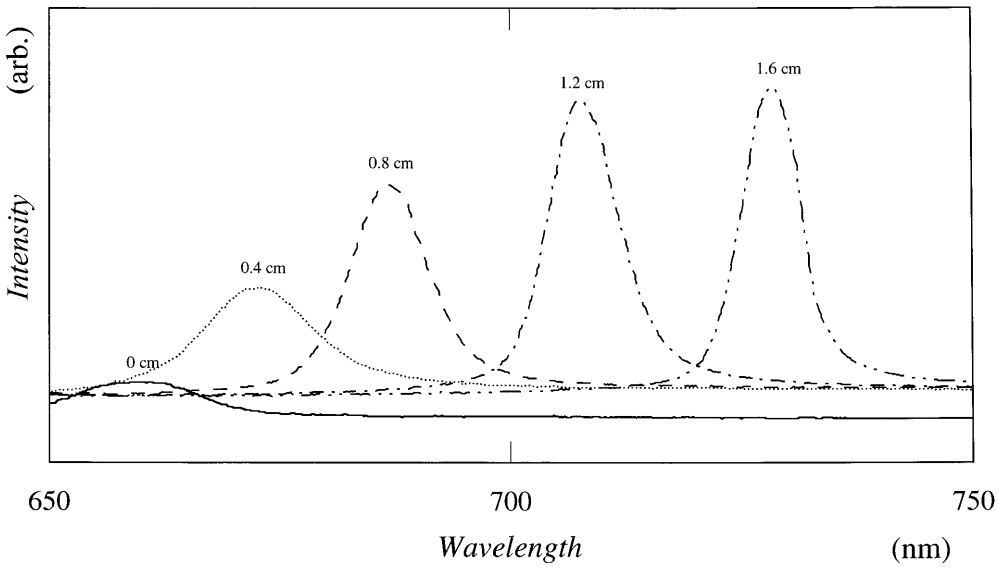


**Fig. 2** Height dependence in the reflection spectra of colloidal crystals of PMMA/$SiO_2$ spheres in acetonitrile and in a sedimentation equilibrium at 25 °C. 21 days after setting the suspension, $\phi = 0.0491$, $M_n = 10000$, $PA = 37$ mg/g$SiO_2$

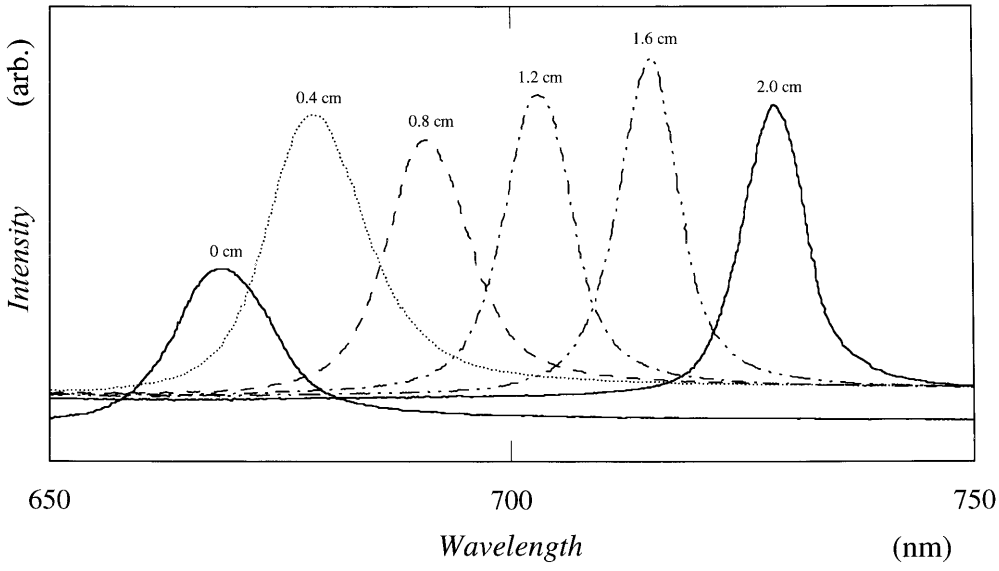


**Fig. 3** Height dependence in the reflection spectra of colloidal crystals of PST/$SiO_2$ spheres in acetonitrile and in a sedimentation equilibrium at 25 °C. 21 days after setting the suspension, $\phi = 0.0862$, $M_n = 11000$, $PA = 17$ mg/g$SiO_2$

double peak, or a single peak with a shoulder [39]. The two peak wavelengths were always close together, with a difference of only 1.027 in the ratios of their wavelengths. The peak appearing at the longer wavelength is ascribed to the face-centered cubic (fcc) lattice, while the shorter wavelength corresponds to the body-centered cubic (bcc) lattice in the crystal structures. All the peak profiles shown in Figs. 1, 2, and 3 showed the single peak. However, the sample suspensions, their codes 4–7, 11, 12, and 14 in Table 1, 4, 21, and 23 in Table 2, and 6 in Table 3 showed the double peak, with a difference of 1.023 (mean value) in the ratio of their peak wavelengths in the reflection spectra. Thus, the peaks appearing at the longer and shorter wavelengths are ascribed to the fcc and bcc lattices, respectively. The nearest-neighbored inter-sphere spacing ($l$) is determined from the peak wavelength for the initial suspension before the sedimentation measurements started [40] and listed in Tables 1, 2, and 3. For both fcc and bcc lattices the distance at a scattering angle of 180° is given by

$$l = 0.6124(\lambda_p / n_s) \tag{1}$$

where $n_s$ is the refractive index of the suspension (taken as that of solvent in this work) and $\lambda_p$ is the peak wavelength.

The mean inter-sphere distance ($l_o$), which is calculated using Eq. (2) when the sphere distribution is the simple-cubic lattice, is

**Table 1** Characteristics of the colloidal crystals of P(MA-ST)/$SiO_2$

| Code | $M_n$ | $PA$ (mg/g $SiO_2$) | $\phi$ | $\lambda_p$ (nm) | $l$ (nm) | $l_o$ (nm) | $G$ (Pa) | $b$ |
|---|---|---|---|---|---|---|---|---|
| 01 | 6700 | 18.0 | 0.0392 | 761.5 | 346 | 362 | 61 | 0.045 |
| 02 | 6700 | 18.0 | 0.0433 | 738.5 | 335 | 350 | 66 | 0.045 |
| 03 | 6700 | 18.0 | 0.054 | 715.6 | 325 | 325 | 82 | 0.045 |
| 04 | 6700 | 18.0 | 0.057 | 699.1 | 317 | 320 | 96 | 0.043 |
| 04 | 6700 | 18.0 | 0.057 | 682.8 | 310 | 320 | 87 | 0.045 |
| 05 | 6700 | 18.0 | 0.068 | 690.0 | 312 | 301 | 130 | 0.041 |
| 05 | 6700 | 18.0 | 0.068 | 671.7 | 304 | 301 | 110 | 0.044 |
| 06 | 6700 | 50 | 0.051 | 719.0 | 326 | 332 | 79 | 0.045 |
| 06 | 6700 | 50 | 0.051 | 699.2 | 317 | 332 | 62 | 0.051 |
| 07 | 6700 | 50 | 0.052 | 701.5 | 318 | 330 | 81 | 0.045 |
| 07 | 6700 | 50 | 0.052 | 685.8 | 311 | 330 | 77 | 0.046 |
| 08 | 6700 | 50 | 0.061 | 675.8 | 306 | 313 | 93 | 0.045 |
| 09 | 6700 | 80 | 0.0408 | 748.0 | 340 | 357 | 59 | 0.047 |
| 10 | 6700 | 80 | 0.0450 | 733.8 | 333 | 346 | 62 | 0.048 |
| 11 | 6700 | 80 | 0.0484 | 723.6 | 328 | 338 | 95 | 0.040 |
| 11 | 6700 | 80 | 0.0484 | 711.7 | 323 | 338 | 73 | 0.045 |
| 12 | 6700 | 80 | 0.066 | 706.0 | 320 | 304 | 110 | 0.043 |
| 12 | 6700 | 80 | 0.066 | 687.2 | 311 | 304 | 95 | 0.047 |
| 13 | 7200 | 90 | 0.0287 | 771.4 | 351 | 401 | 40 | 0.047 |
| 14 | 7200 | 90 | 0.0354 | 766.0 | 348 | 374 | 64 | 0.042 |
| 14 | 7200 | 90 | 0.0354 | 748.2 | 340 | 374 | 58 | 0.044 |
| 15 | 7200 | 90 | 0.0362 | 788.0 | 358 | 372 | 70 | 0.040 |

**Table 2** Characteristics of the colloidal crystals of PMMA/$SiO_2$

| Code | $M_n$ | $PA$ (mg/g$SiO_2$) | $\phi$ | $\lambda_p$ (nm) | $l$ (nm) | $l_o$ (nm) | $G$ (Pa) | $b$ |
|---|---|---|---|---|---|---|---|---|
| 01 | 5100 | 14.6 | 0.0416 | 714.4 | 325 | 355 | 59 | 0.047 |
| 02 | 5100 | 14.6 | 0.084 | 612.2 | 277 | 281 | 330 | 0.028 |
| 03 | 5100 | 34.7 | 0.0329 | 758.5 | 345 | 384 | 48 | 0.046 |
| 04 | 5100 | 34.7 | 0.0492 | 734.9 | 334 | 336 | 100 | 0.039 |
| 04 | 5100 | 34.7 | 0.0492 | 722.6 | 328 | 336 | 83 | 0.043 |
| 05 | 5100 | 34.7 | 0.096 | 579.5 | 262 | 268 | 430 | 0.027 |
| 06 | 8000 | 17.8 | 0.0442 | 760.9 | 346 | 348 | 71 | 0.044 |
| 07 | 8000 | 17.8 | 0.094 | 603.0 | 272 | 270 | 430 | 0.026 |
| 08 | 8000 | 35.8 | 0.0412 | 761.4 | 346 | 356 | 65 | 0.045 |
| 09 | 8000 | 35.8 | 0.107 | 580.2 | 262 | 259 | 330 | 0.032 |
| 10 | 10000 | 37.0 | 0.0390 | 753.6 | 342 | 363 | 73 | 0.041 |
| 11 | 10000 | 37.0 | 0.0490 | 698.8 | 317 | 336 | 110 | 0.038 |
| 12 | 10000 | 37.0 | 0.071 | 620.3 | 281 | 296 | 280 | 0.028 |
| 13 | 10000 | 55 | 0.0357 | 764.7 | 348 | 373 | 62 | 0.042 |
| 14 | 10000 | 55 | 0.066 | 653.7 | 296 | 304 | 340 | 0.024 |
| 15 | 10800 | 40.5 | 0.059 | 664.0 | 301 | 315 | 110 | 0.042 |
| 16 | 11000 | 49.8 | 0.0471 | 746.3 | 339 | 340 | 75 | 0.044 |
| 17 | 12000 | 56 | 0.050 | 720.8 | 262 | 285 | 92 | 0.041 |
| 18 | 15000 | 16.0 | 0.0353 | 778.3 | 354 | 375 | 56 | 0.045 |
| 19 | 15000 | 16.0 | 0.102 | 592.3 | 267 | 263 | 300 | 0.033 |
| 20 | 15000 | 32.9 | 0.0475 | 761.3 | 346 | 340 | 73 | 0.045 |
| 21 | 15000 | 69 | 0.066 | 657.6 | 298 | 304 | 110 | 0.043 |
| 21 | 15000 | 69 | 0.066 | 643.4 | 291 | 304 | 100 | 0.045 |
| 22 | 15000 | 147 | 0.0396 | 706.4 | 321 | 361 | 65 | 0.044 |
| 23 | 15000 | 147 | 0.067 | 636.1 | 288 | 303 | 120 | 0.042 |
| 23 | 15000 | 147 | 0.067 | 621.2 | 281 | 303 | 110 | 0.044 |
| 24 | 21300 | 53 | 0.0470 | 768.9 | 349 | 341 | 68 | 0.047 |

$$l_0 = 0.904 d_0 \phi^{-1/3} \quad (2)$$

where the refractive indices were taken to be 1.33, 1.34, 1.55, and 1.50 for water, acetonitrile, nitrobenzene, and silica spheres, respectively. Furthermore, the $d_o$ value was taken as 136 nm for the size of the mother silica spheres, since the real size of the spheres including the polymer layers is difficult to estimate in this work. The values of $l$ and $l_o$ are listed in Table 1. The $l$ and $l_o$-values are also plotted against the logarithm of the number

**Table 3** Characteristics of the colloidal crystals of PST/$SiO_2$

| Code | $M_n$ | $PA$ (mg/g$SiO_2$) | $\phi$ | $\lambda_p$ (nm) | $l$ (nm) | $l_o$ (nm) | $G$ (Pa) | $b$ |
|---|---|---|---|---|---|---|---|---|
| 01 | 11000 | 17.1 | 0.086 | 702.6 | 278 | 278 | 200 | 0.037 |
| 02 | 11000 | 17.1 | 0.091 | 672.7 | 267 | 274 | 250 | 0.034 |
| 03 | 11000 | 34.4 | 0.087 | 690.1 | 273 | 278 | 230 | 0.035 |
| 04 | 11000 | 34.4 | 0.098 | 651.3 | 258 | 267 | 260 | 0.035 |
| 05 | 16000 | 25.8 | 0.087 | 688.6 | 273 | 277 | 190 | 0.038 |
| 06 | 16000 | 25.8 | 0.091 | 680.3 | 270 | 274 | 160 | 0.042 |
| 06 | 16000 | 25.8 | 0.091 | 666.2 | 264 | 274 | 190 | 0.039 |
| 07 | 28000 | 18.1 | 0.073 | 727.5 | 288 | 294 | 130 | 0.042 |
| 08 | 28000 | 18.1 | 0.097 | 648.4 | 257 | 268 | 220 | 0.037 |
| 09 | 28000 | 29.3 | 0.063 | 776.4 | 307 | 310 | 110 | 0.042 |
| 10 | 28000 | 29.3 | 0.100 | 651.2 | 258 | 265 | 230 | 0.037 |

density ($N$) of spheres in Figs. 6a, 7a, and 8a, for P(MA-ST)/$SiO_2$, PMMA/$SiO_2$, and PST/$SiO_2$ systems, respectively. Clearly, agreement between $l$ and $l_o$ was excellent when the experimental errors were taken into account.

## Rigidity of colloidal crystals

The lattice spacing, $l$ is given by Eq. (3) in the sedimentation equilibrium [41]:

$$l - l_m = \left(\rho_{eff} g l_m \phi_m / G\right)(h - h_m) \tag{3}$$

where $l_m$ and $\phi_m$ indicate the lattice spacing and the sphere concentration at the midplane, $h_m$, respectively. $\phi_m$ is therefore equal to the initial concentration, $\phi$ in Tables 1, 2, and 3. $\rho_{eff}$ is the effective density given by the specific gravity of spheres minus that of the solvent, and $g$ is the gravitational constant. $G$ is the Young's elastic modulus (rigidity) for the colloidal crystals and obtained from the slopes of $l$ (or reflection peak wavelength, $\lambda_p$ using Eq. (1) vs $h$ plots shown in Fig. 4, for example. The linearity was excellent except the data at the top and bottom layers of the suspensions. The values of $G$ thus estimated are compiled in Tables 1, 2, and 3.

Logarithms of $G$-values of the colloidal crystals are shown as a function of log $N$ in Figs. 6b, 7b, and 8b, for P(MA-ST)/$SiO_2$, PMMA/$SiO_2$, and PST/$SiO_2$ systems, respectively. The order of magnitude of $G$ is written in terms of the magnitude of the thermal fluctuation $\delta$ of a sphere as [5, 14]:

$$G \sim f/l \sim \left(k_B T/\delta^2\right)/l \tag{4}$$

where $f$ is the force constant, and $\delta$ is the thermal fluctuation of a sphere in the effective potential valley. Introducing a non-dimensional parameter $b$ for $<\delta^2>^{1/2}/l$, the modulus is obtained as a linear function of $N$:

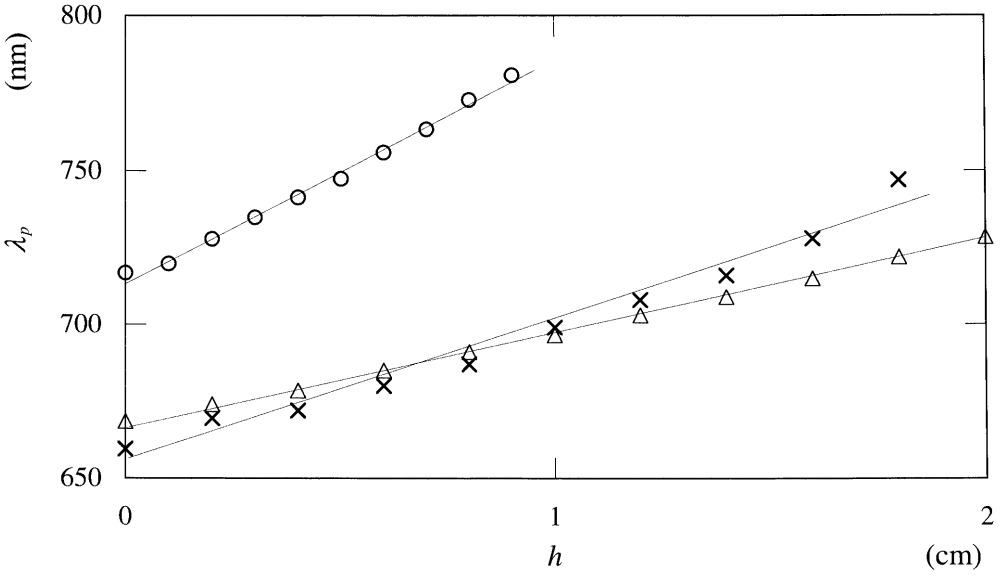


**Fig. 4** Peak wavelengths plotted against heights at 25 °C. 21 days after setting the suspension, *open circles*: P(MA-ST), $\phi$ = 0.0408, $M_n$ = 6700, PA = 80 mg/g$SiO_2$, *crosses*: PMMA, 0.0491, 10000, 37, *open triangles*: PST, 0.0862, 11000, 17

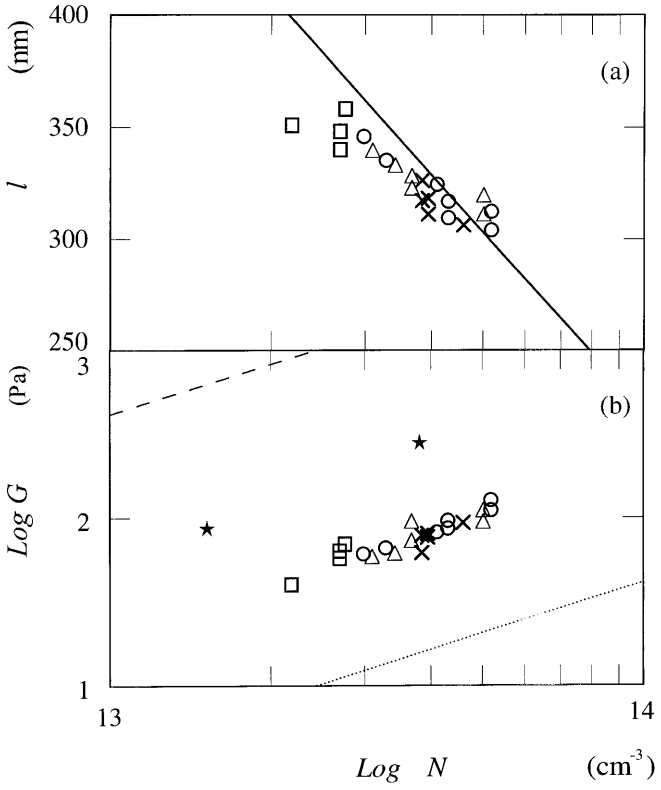


**Fig. 5** **a** *l*. **b** log *G* of P(MA-ST)/$SiO_2$ spheres plotted against log *N*, in acetonitrile at 25 °C. *Open circles*: $M_n = 6700$, $PA = 18$ mg/g$SiO_2$, *crosses*: 6700, 50, *open triangles*: 6700, 80, *open squares*: 7200, 90, *stars*: mother silica in water. *Solid line* in (a) shows the calculation, *dotted and broken lines* in (b) show the calculation at $b = 0.1$, and 0.01, respectively

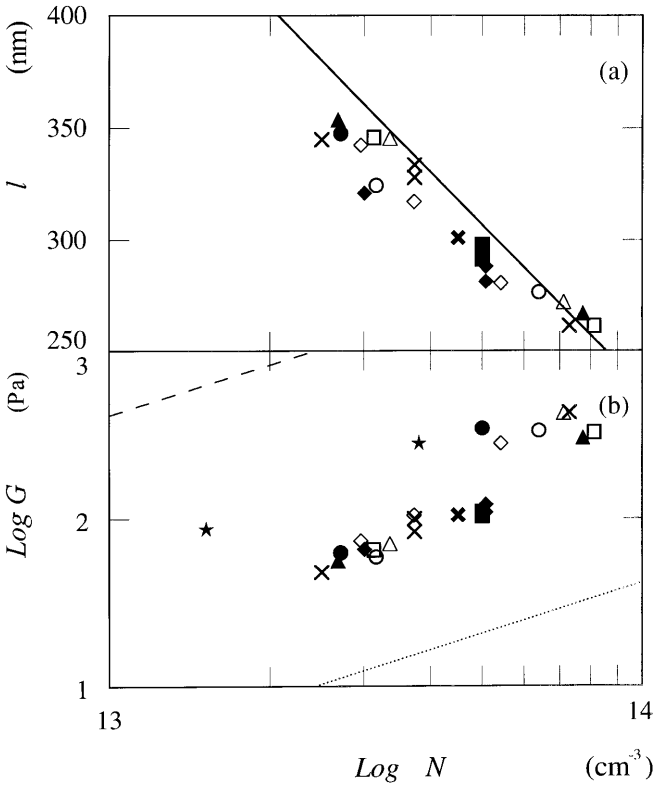


**Fig. 6** **a** *l*. **b** log *G* of PMMA/$SiO_2$ spheres plotted against log *N* in acetonitrile at 25 °C. *Open circles*: $M_n = 5100$, $PA = 14.6$ mg/g$SiO_2$, *light crosses*: 5100, 34.7, *open triangles*: 8000, 17.8, *open squares*: 8000, 35.8, *open lozenges*: 10000, 37, *filled circles*: 10000 55, *bold crosses*: 10800, 40.5, *filled triangles*: 15000, 16, *filled squares*: 15000, 69, *filled lozenges*: 15000, 147, *stars*: mother silica in water. *Solid line* in (a) shows the calculation, *dotted and broken lines* in (b) show the calculation at $b = 0.1$, and 0.01, respectively

$$G \sim Nk_BT/b^2 \tag{5}$$

When $b = 1$, Eq. (5) gives the elastic modulus of an ideal gas having the same sphere concentration. Lindemann's law of crystal melting tells us that $b < 0.1$ holds for a stable crystal. The dotted and broken lines in Figs. 5, 6, and 7 represent the values of *G* when $b = 0.1$ and 0.01, respectively. Clearly, all the *G* values in the figures are located between the dotted and broken lines. The *b*-values estimated are also compiled in Tables 1, 2, and 3, and $0.045 \pm 0.003$, $0.039 \pm 0.007$, and $0.038 \pm 0.003$, for P(MA-ST)/$SiO_2$, PMMA/$SiO_2$, and PST/$SiO_2$ systems, respectively.

## Comparison of the excluded volume effects from the polymer layers and from the electrical double layers

Generally speaking, most colloidal particles in aqueous and polar organic solvents acquire negative charges on their surfaces by two mechanisms: one is dissociation of ionizable groups and the other is preferential adsorption of ions from suspension. Typical examples are gold and silver particles, which are neutral but negatively charged on their surfaces. It should be noted that many simple ions are oppositely charged, and distribute around the negatively charged colloidal particles. The region where small ions distribute is called the *electrical double layer*.

Thickness of the electrical double layers is approximated with the Debye-screening length, $D_l$, given by Eq. (6):

$$D_l = \left(4\pi e^2 n/\varepsilon k_B T\right)^{-1/2} \tag{6}$$

where *e* is the electronic charge and $\epsilon$ is the dielectric constant of the solvent. *n* is the concentration of "diffusible" or "free-state" cations and anions in suspension. Thus, *n* is the sum of the concentrations of diffusible counterions, foreign salt, and both $H^+$ and $OH^-$ from the dissociation of water. The maximum value of $D_l$ in water is ca. 1 μm, which is estimated from Eq. (6) by taking $n = 2\times10^{-7}$ (mol/dm$^3$)$\times N_A \times 10^{-3}$ cm$^{-3}$,

where $N_A$ is Avogadro's number. It should be noted that electrical double layers are formed, without exception, in the solid-in-polar liquid type colloidal suspension.

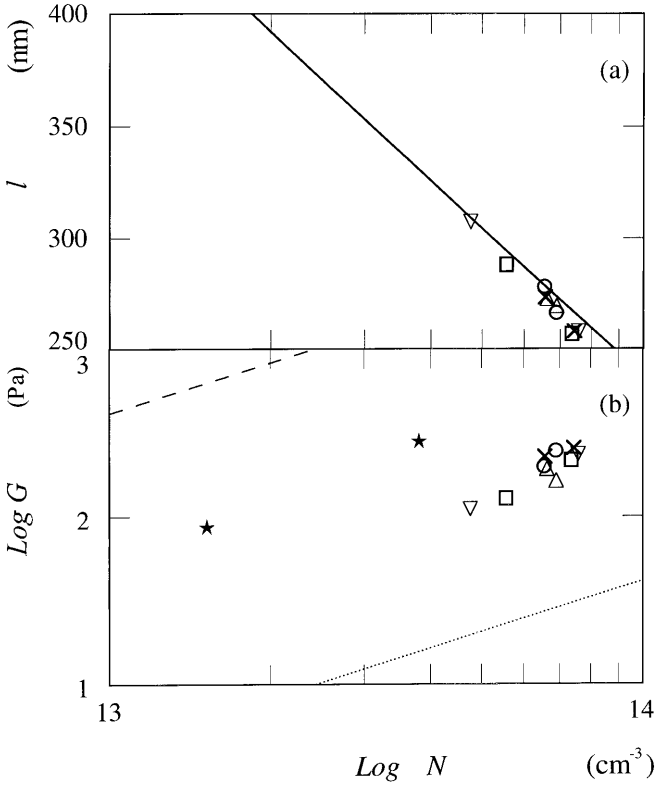


**Fig. 7** **a** $l$. **b** log $G$ of PST/$SiO_2$ spheres plotted against log $N$ in acetonitrile at 25 °C. *Open circles*: $M_n = 11000$, $PA = 17.1$ mg/g$SiO_2$, *crosses*: 11000, 34.4, *open triangles*: 16000, 25.8, *open squares*: 28000, 18.1, *open lozenges*: 28000, 29.3, **stars**: mother silica in water. *Solid line* in (a) shows the calculation, *dotted and broken lines* in (b) show the calculation at $b = 0.1$, and 0.01, respectively

The colloidal crystallization in aqueous and polar organic solvents is explained nicely with the *effective soft-sphere model*. The effective diameter, $d_{eff}$ of spheres includes the electrical double layers, which is approximated with the Debye-screening length, $D_l$ described above and given by the diameter plus twice the polymer layer's thickness and further plus twice the Debye length (see Eq. 7):

$$d_{eff} = d_0 + 2\sigma + 2D_l \tag{7}$$

where $\sigma$ is the thickness of the polymer layers. For the colloidal crystallization of the mother colloidal silica spheres $\sigma$ is zero. When $d_{eff}$ is shorter than the observed intersphere distance, $l$, a gas-like distribution is observed. When $d_{eff}$ is comparable to or a bit shorter than the intersphere distance, the distribution of spheres is usually liquid-like. When the effective diameter is close to or larger than the observed intersphere distance, crystal-like ordering is formed. This *effective soft-sphere model* has been supported, especially for aqueous suspensions of colloidal spheres without polymer layers, i.e., $\sigma = 0$ by many researchers from the systematic comparison between $d_{eff}$ and $l$ values [11, 14].

The magnitudes of the thickness of the polymer layers ($\sigma$) when their conformations are random coil (solid symbols) or extended (open symbols) on the colloidal silica surfaces are shown in Fig. 8, and compared with the values of the total excluded layer's thickness for crystallization, $\sigma + D_l$. The polymers of P(MA-ST) in acetonitrile, PMMA in acetonitrile, and PST in nitrobenzene will be rather extended, since the corresponding solvents are good solvent for each polymers and there exists the repulsion between the neighboring polymers attached on the colloidal surfaces. The $\sigma$-values of the three systems in Fig. 8 seem to be in the order (Eq. 8):

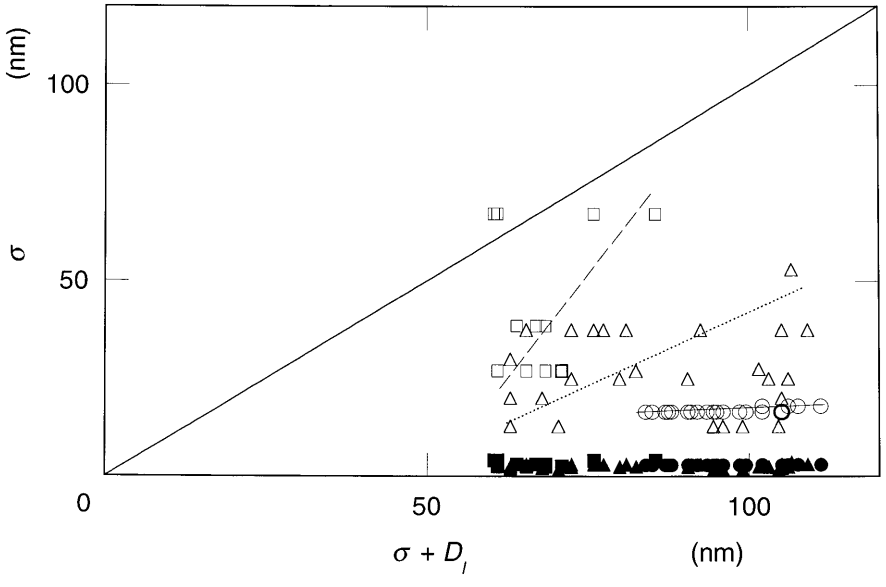


**Fig. 8** The evaluated thickness of the adsorption layers compared with the maximum thickness for the colloidal crystals of P(MA-ST)/$SiO_2$ (*open circles, filled circles*), PMMA/$SiO_2$ (*open triangles, filled triangles*), and PST/$SiO_2$ (*open squares, filled squares*). *Open and solid symbols* show the thickness when the polymers are extended and coil, respectively

$$P(MA-ST)/SiO_2 < PMMA/SiO_2 < PST/SiO_2. \quad (8)$$

The dielectric constants of acetonitrile and nitrobenzene are 37.5 and 35.7 at 20 °C, respectively. These organic solvents are, therefore, rather highly polar solvents, and contribution of the $D_l$-term should be significant for the colloidal crystallization, though the $D_l$ in the organic solvents is certainly smaller than that of the mother silica spheres in aqueous deionized suspensions. Quantitative discussion of the $D_l$-values is quite difficult for our systems, since the effective charge number dissociated on the colloidal sphere surfaces and then the $n$-values in Eq. (6) are unknown. Furthermore, the organic solvents, acetonitrile and nitrobenzene, were used without further deionization treatment with the mixed beds of cation- and anion-exchange resins, for example, and contain a small amount of the ionic impurities in the suspensions. However, it is concluded that the *excluded volume effects* from the polymer layers and the electrical double layers play an important role for the colloidal crystallization.

**Acknowledgments** Drs M. Komatsu, H. Nishida, and M. Hirai of Catalysts & Chemicals Ind. Co. (Tokyo and Kitakyusyu) are sincerely thanked for providing the silica samples. Professor Akira Tsuchida of Gifu University is acknowledged for his valuable comments. The Ministry of Education, Science, Sports and Culture is thanked for Grants-in-Aid for Scientific Research on Priority Area (A) (11167241) and for Scientific Research (B) (11450367). T.O. thanks the late Professor Emeritus Sei Hachisu for his continual encouragement and comments on our work on colloidal crystals.

## References

1. Vanderhoff W, van de Hul HJ, Tausk RJM, Overbeek JTG (1970) Clean surfaces: their preparation and characterization for interfacial studies. Goldfinger G (ed). Dekker, New York
2. Hiltner PA, Papir YS, Krieger IM (1971) J Phys Chem 75:1881
3. Kose A, Ozaki M, Takano K, Kobayashi Y, Hachisu S (1973) J Colloid Interface Sci 44:330
4. Williams R, Crandall RS, Wojtowicz PJ (1976) Phys Rev Lett 37:348
5. Mitaku S, Ohtsuki T, Kishimoto A, Okano K (1980) Biophys Chem 11:411
6. Lindsay HM, Chaikin PM (1982) J Chem Phys 76:3774
7. Pieranski P (1983) Contemp Phys 24:25
8. Ottewill RH (1985) Ber Bunsenges Phys Chem 89:517
9. Aastuen DJW, Clark NA, Cotter LK, Ackerson BJ (1986) Phys Rev Lett 57:1733
10. Pusey PN, van Megen W (1986) Nature (London) 320:340
11. Okubo T (1988) Acc Chem Res 21:281
12. Russel WB, Saville DA, Schowalter WR (1989) Colloidal dispersions. Cambridge University Press, Cambridge
13. Stevens MJ, Falk ML, Robins MO (1966) J Chem Phys 104:5209
14. Okubo T (1993) Prog Polymer Sci (1993) 18:481
15. Okubo T (1994) Macro-ion characterization. from dilute solutions to complex fluids. Schmitz KS (ed). ACS Symp Ser 548, Am Chem Soc, Washington DC, pp 364–380
16. Okubo T (1997) Curr Top Colloid Interface Sci 1:169
17. Okubo T (2002) Encyclopedia of surface and colloid science. Hubbard A (ed). American Chemical Society, Washington DC (in press)
18. Okubo T (1987) J Chem Phys 86:2394
19. Okubo T (1987) J Chem Phys 86:5182
20. Okubo T (1987) J Chem Phys 87:3022
21. Okubo T (1987) J Chem Soc Faraday Trans 1 83:2487
22. Okubo T (1987) Angew Chem Intern Ed Engl 26:765
23. Okubo T (1987) Colloid Polym Sci 265:522
24. Okubo T, Aotani S (1988) Colloid Polym Sci 266:1042
25. Okubo T, Aotani S (1988) Colloid Polym Sci 266:1049
26. Okubo T (1989) J Chem Soc Faraday Trans 1 85:455
27. Okubo T (1990) J Chem Phys 93:8276
28. Okubo T (1990) J Am Chem Soc 112:5420
29. Okubo T (1990) J Colloid Interface Sci 135:259
30. Okubo T (1990) Colloid Polym Sci 268:1159
31. Matsumoto T, Okubo T (1991) J Rheol 35:135
32. Okubo T (1993) Colloid Polym Sci 271:873
33. Okubo T (1995) J Chem Phys 102:7721
34. Okubo T (1988) J Chem Phys 88:2083
35. Okubo T (1990) J Chem Soc Faraday Trans 86:151
36. Lekkerkerker HNW, Dhont JKG, Verduin H, Smits C, Vanduijneveldt JS (1995) Physica A 213:18
37. Watzlawek M, Likos CN, Lowen H (1999) Phys Rev Lett 82:5289
38. Yoshinaga K, Nakanishi K (1994) Compos Interf 2:95
39. Okubo T (1986) J Chem Soc Faraday Trans 1 82:3163
40. Okubo T (1988) J Colloid Interface Sci 125:380
41. Crandall RS, Williams R (1977) Science 198:293